

PRESSURE DROP AND FLOW BEHAVIOUR OF REFRIGERANT TWO PHASE FLOW IN A SMOOTH HAIRPIN

De Kerpel K.*, Ameel B., Canière H. and De Paepe M.

*Author for correspondence

Department of Flow, Heat and Combustion Mechanics,

Ghent University - UGent,

Sint-Pietersnieuwstraat 41,

9000 Ghent

Belgium,

E-mail: Kathleen.DeKerpel@Ugent.be

ABSTRACT

Two-phase flow of refrigerant R134a in a hairpin was studied. The hairpin consists of a smooth tube with an inner diameter of 8mm with a U-bend radius of 11mm. Because of the forces exerted on the flow in the U-bend the flow needs to develop again downstream of the U-bend. The effects of this phenomenon on the pressure drop are studied and linked to a visual observation of the flow. Pressure drop and videos of the flow are recorded in the straight sections upstream and downstream of the U-bend. Afterwards they are compared to the flow and pressure drop for developed flow. The pressure drop downstream of the U-bend was found to be consistently higher than that for developed flow. It exceeded the pressure drop in case of developed flow by an average of 30% for all data points. Each video of the flow behaviour was reduced to a single image by calculating the standard deviation of the time signal per pixel in time. The standard deviation profiles were compared in order to quantitatively evaluate the change in the flow behaviour. For the flow downstream of the U-bend a disturbance was observed that stretches out over more than 30 diameters downstream of the U-bend.

INTRODUCTION

Two-phase refrigerant flow has already been the subject of extensive research. Most of this research is focused on developed two-phase flow in a straight tube, yet this condition only occurs in a small section of some types of heat exchangers, such as air conditioning units. This is due to the geometry: fin-and-tube heat exchangers consist of a series of straight tubes linked with U-bends, called hairpins. The disturbance of the flow resulting from the presence of these bends is not limited to the U-bend itself but it extends to the straight sections of the hairpin. As a result, the correlations for pressure drop and heat transfer coefficient for developed flow in a straight tube are not accurate for hairpins since the pressure drop and heat transfer are strongly influenced by the flow behaviour induced by the U-bend. These 'U-bend effects' have been investigated by Ribeiro et al. [1] and Wang et al. [2, 3],

though the results of these studies are still too limited to allow for a more efficient design of heat exchangers.

In the available studies air-water mixtures were used. The thermo physical properties of R134a differ from these of an air-water mixture. Furthermore, an air water mixture does not show a saturation equilibrium between two phases of the same substance, as is the case for two phase flow of a refrigerant. Hence, results might not be applicable to two-phase refrigerant flow [4, 5].

For the pressure drop in U-bends many correlations have been developed [6-10] based on refrigerant flow measurements. However, these correlations do not provide an estimation of the pressure drop in the straight sections of a hairpin, where the flow is developing downstream of the U-bend. Furthermore, none of the cited studies provide a coupling between the observed flow behaviour and the measured pressure drop, in spite of their explicit interrelation. The aim of this work is to investigate the flow behaviour of R134a in a hairpin, focusing on the impact of the U-bend, the developing flow downstream, and to quantify the impact of the U-bend on the pressure drop in the downstream straight tube sections of a hairpin.

NOMENCLATURE

D	[m]	Tube diameter
G	[kg/m ² s]	Mass flux
ΔP	[Pa]	Pressure drop
R	[m]	U-bend radius
T	[°C]	Temperature
x	[-]	Vapour quality

Special characters		
σ	[-]	Standard deviation

Subscripts		
<i>dev</i>		Developed flow
<i>downstream</i>		Immediately downstream of the U-bend
<i>upstream</i>		Immediately upstream of the U-bend
<i>sat</i>		saturation

EXPERIMENTAL SETUP

The experimental setup comprises a refrigerant loop, a hot water loop and a cold water loop. In Figure 1 only the refrigerant loop is shown. This setup was previously developed for the study of two phase refrigerant flow in straight tubes, more information can be found in Canière et al. [11-13]. The preheater is a tube-in-tube heat exchanger; its length can be varied between 1 and 15 m by adjusting shut-off valves. Water from the hot water loop flows through the annulus of the preheater, transferring heat to the coolant flowing in the inner tube which will start to evaporate. By changing the length of the preheater, the inlet temperature and mass flow rate of the hot water in the annulus, the vapour quality at the preheater outlet can be controlled.

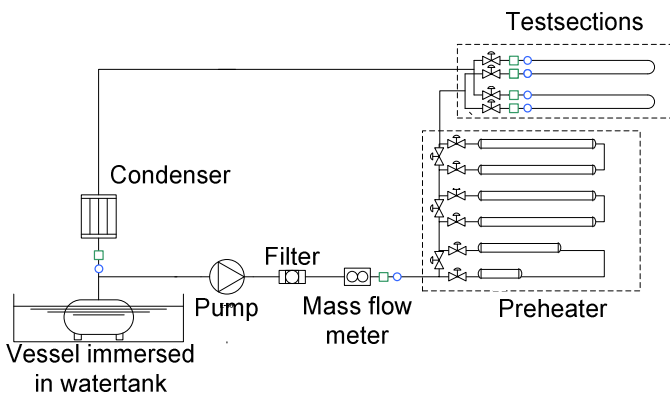


Figure 1 Schematic of the refrigerant loop

After the preheater the refrigerant flows through the test sections, of which the first 140D are used as a settling length. Each of the two test section consists of a hairpin with a bend radius R of 11mm and an inner diameter ID of 8mm. The orientation of the U-bend is vertical, and the refrigerant flows downwards from the top tube to the bottom tube. The inner tube wall is smooth and both test sections are adiabatic. One test section is used for pressure measurements and the one for recording the videos of the flow behaviour. Pressure drop and flow behaviour are recorded immediately upstream and downstream of the U-bend to register possible U-bend effects and also at a sufficient distance (130 diameters) upstream (developed) of the U-bend.

The pressure drops are measured over a length of 0.2m. The differential pressure transducer has a range of 0-50kPa and an accuracy of 0.2mbar. The test section for flow observation is a hairpin made out of quartz glass. The flow is filmed with a monochromatic camera (Basler A602f - 640x480 pixels).

A vessel immersed in an open water bath is connected to the refrigerant loop between the condenser and the preheater. As a liquid-vapour interface exists in the vessel, the refrigerant saturation temperature $T_{sat,ref}$ is fixed by the temperature of the water surrounding the vessel. $T_{sat,ref}$ is set at 15°C for all measurements.

VISUAL OBSERVATION OF THE FLOW BEHAVIOUR

Each flow visualisation consists of 2000 frames. In order to easily visualize the effect of the U-bend on the flow behaviour, the recorded videos of the two phase flow are converted into a

single image. To this end the standard deviation of the fluctuating pixel intensity is computed and shown for each pixel. Areas with high standard deviation (strong fluctuations) are coloured white, black zones indicate little or no variation in time. Hence black zones are either background or zones where consistently only a single phase is present. White zones however exhibit a large amount of interfacial activity. By evaluating the standard deviation, it can be easily visualised and determined how far the effect of the U-bend extend downstream of the U-bend in the straight section.

Slug flow regime

Figure 2 shows the standard deviation plots for $G=200$ kg/m²s and $x=1\%$; the fully developed flow regime is slug flow. Upstream of the U-bend, a large black zone near the bottom is noticeable. This zone is filled with fluid phase at each moment in time (zone 1, Fig. 2b), there is little interfacial activity resulting in a low standard deviation. Above this black zone, a white zone is apparent; this high standard deviation is caused by the liquid-vapour interface which disappears when a slug is passing by (zone 2, Fig. 2b). The gray zone above it is a zone that consists of vapour phase most of the time, it only shows an interface when the edges of a slug are passing by (zone 3, Fig. 2b).

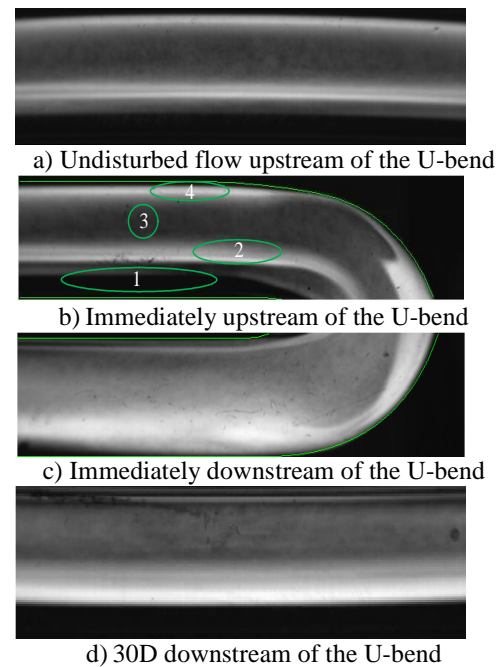
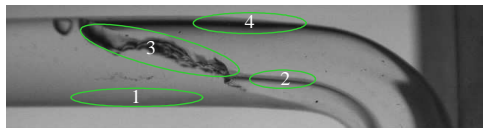


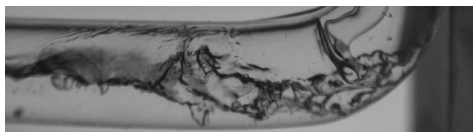
Figure 2 Standard deviation plot for $G=200$ kg/m²s, $x=1\%$

At the very top of the straight section of the tube another white zone can be seen. This zone has a low pixel intensity when vapour is present and has a high pixel intensity when a liquid slug is passing by, resulting in high standard deviation (zone 4, Fig. 2b). This effect is due to optical refraction. The refractive index of the glass is about 1.4, that of the liquid is in the order of 1.2 and that of the vapour 1.007. Because of the larger difference in refractive index between glass and vapour, the rays of light passing through the upper tube wall to the

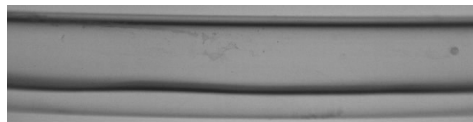
camera lens do not come from the backlight; hence the pixel intensity is low. When there is liquid present, the refraction is smaller and the rays of light illuminating the upper tube wall do come from the backlight causing the pixel intensity to be higher. This effect could be avoided by using two additional backlights: one above and one underneath the hairpin. However, this would also reduce the effects of optical refraction at the interface between the two phases due to which the vapour-liquid interface would be less visible on the images.



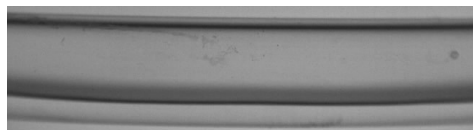
a) Immediately upstream of the U-bend



b) Immediately downstream of the U-bend



c) 30D downstream of the U-bend



d) 30D downstream of the U-bend at another instance in time

Figure 3 Images of the flow behaviour for $G=200 \text{ kg/m}^2\text{s}$, $x=1\%$

The zones in Figure 2 are also indicated in Figure 3, which contains actual time frames from the videos, showing the flow mechanisms responsible for the observed variations of the standard deviation.

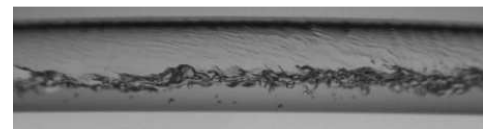
It is very clear from the standard deviation plots (Fig. 2) that the flow in the straight section downstream of the U-bend is fundamentally different from the flow upstream of the U-bend. This is also evident when one looks at unprocessed images of the flow behaviour itself. Figure 3b shows a slug approaching the U-bend and Error! Reference source not found.c shows the flow after a slug has just passed through the U-bend. These are only snapshots; the flow shows significant variation in time. The standard deviation however synthesises the video in a single image, which allows for an easy comparison between the flows at different axial positions.

Figure 2 reveals several more phenomena. Firstly, in the top image showing the flow upstream of the U-bend, there is little or no axial variation in the standard deviation in the straight section. This is also the case for fully developed flow.

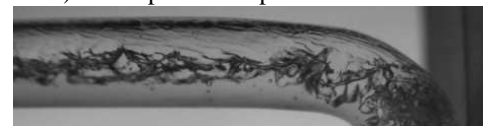
However, in the bottom image showing the flow downstream of the U-bend, the standard deviation in the straight section is completely different from the straight section upstream the U-bend. Also, a clear axial variation is visible; which is typical for developing flow. In the bottom left corner of Fig. 2c, the beginning of a black zone can be observed, corresponding to a zone which only shows the liquid phase. Looking further downstream of the U-bend, the figure of the standard deviation is expected to show more similarity to the plot upstream the U-bend. This is confirmed in Figure 3d, which shows a straight section 30 diameters downstream of the U-bend. In that image, zone 1 with only liquid can again be seen. Zone 2, which represents the position of the liquid-vapour phase, is still a lot wider than it was before the bend. In order to find a physical explanation, the fluctuations of the flow must be observed. As evidenced by Figure 3c) and d), the liquid-vapour interface moves in time. This is caused by an oscillatory motion of the liquid phase, a wavy interface. This movement of the interface is significantly more noticeable in the developing case than in the fully developed case, which results in a wider band of high standard deviation. For these conditions the flow still is not fully developed after 30 tube diameters.

Intermittent flow regime

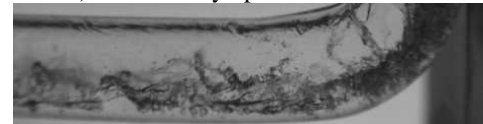
The next flow regime to be analysed is that of intermittent flow ($G=320 \text{ kg/m}^2\text{s}$, $x=15\%$). Figure 4 shows timeframes of the flow up- and downstream of the U-bend. Again the flow is significantly different at both locations. The flow upstream of the bend shows hardly any difference compared to the fully developed flow. This is further illustrated in Figure 5. Both Figure 5a and b show very similar trends for the standard deviation.



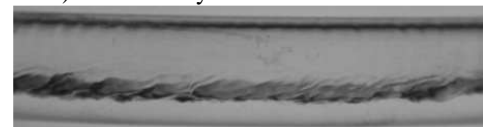
a) developed flow upstream of the U-bend



b) Immediately upstream of the U-bend



c) Immediately downstream of the U-bend



d) 30D downstream of the U-bend

Figure 4 Images of the flow behaviour for $G=320 \text{ kg/m}^2\text{s}$, $x=15\%$

Figure 5c, showing the standard deviation plot of the flow directly downstream, is quite different from the flow upstream. One immediately notices that the black zone is missing, similar as for slug flow. The axial variation is also quite clear. In Figure 5d the standard deviation plot of the flow 30 diameters downstream of the U-bend is shown.

Figure 5d shows that the black zone indicating liquid flow has been restored further downstream of the U-bend. However, when Figure 5d is compared to Figure 5a, the flow behaviour 30 diameters downstream exhibits a more concentrated white zone directly above the black zone, which is not present in the fully developed flow. This is due to the different behaviour of the liquid- vapour interface, as can be seen in Figure 4. The interfacial waves in the developing region downstream the bend have a smaller average amplitude; less of these waves reach the top of the tube compared to the flow behaviour upstream of the U-bend. Hence, the interfacial activity is more concentrated.

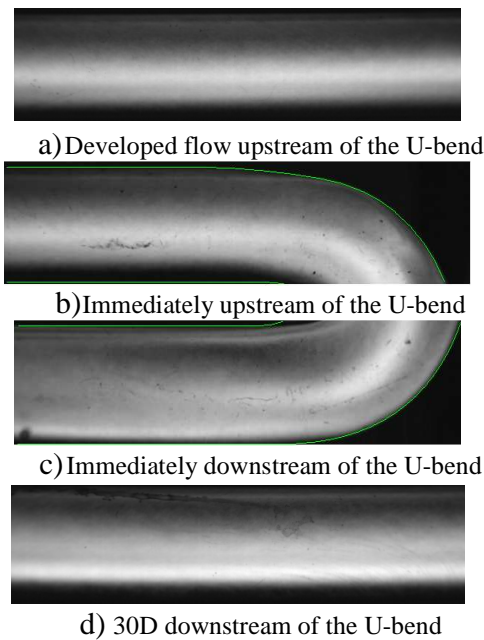


Figure 5 Standard deviation plots for $G=320 \text{ kg/m}^2\text{s}$, $x=15\%$

Obviously the presented flows are highly unsteady, which makes it difficult to represent the flow with single images. In Figure 4 an instant was chosen that is representative for a significant period of time.

Annular flow regime

The final flow regime which was considered is that of annular flow ($G=205 \text{ kg/m}^2\text{s}$, $x=90\%$). Figure 6 shows timeframes of the flow up- and downstream of the U-bend. The difference in flow behaviour is a lot less obvious than in the previous cases. On the inside of the bottom part of the bend, visible in Figure 7c there is noticeably more interfacial activity. In the flow visualisations it can be seen that in the U-bend liquid moves towards the outer wall of the bend. At the outlet of the bend the liquid that has not reached the outside wall seems to be pushed to the upper wall of the outlet straight

section by the vapour core. Figure 7 shows the corresponding standard deviations.

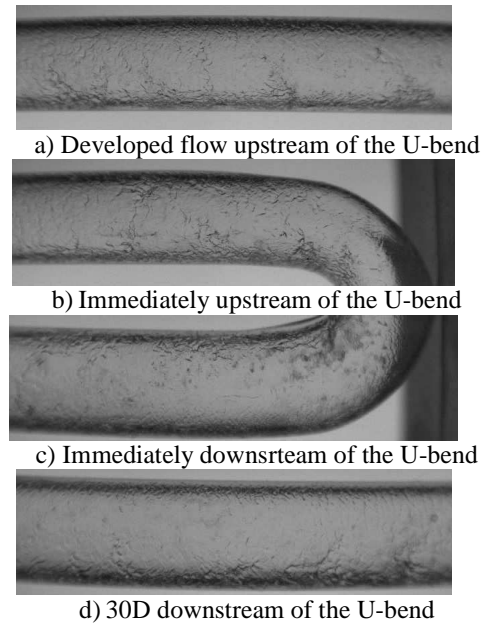


Figure 6 Images of the flow behaviour for $G=205 \text{ kg/m}^2\text{s}$, $x=90\%$.

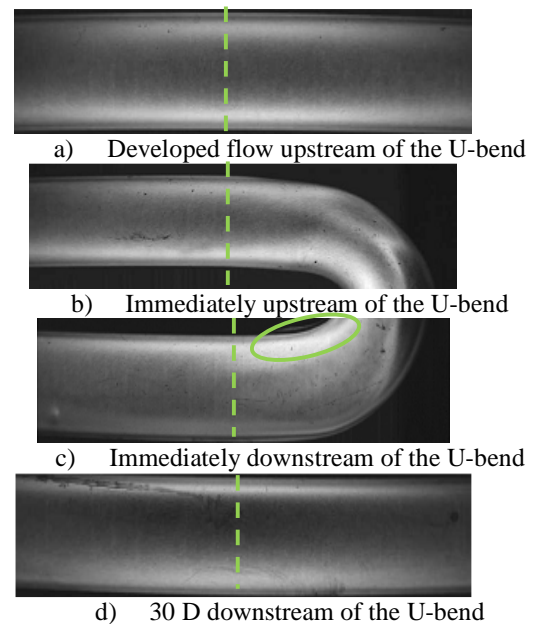


Figure 7 Standard deviation plots for $G=205 \text{ kg/m}^2\text{s}$, $x=90\%$.

The increased interfacial activity on the inside of the U-bend is very apparent in Figure 7c. The straight section upstream of the U-bend shows little or no difference with the fully developed flow, similar to the previously studied flow regimes. Furthermore, the standard deviation plot of the flow

downstream again shows axial variation, indicative of developing flow.

Since the differences between the plots in Figure 7 are not as pronounced as for the previous flows, the standard deviation will be used quantitatively. For this reason the values of the standard deviation along the middle column of Figure 7 are shown in . Between rows 0 to 20 and rows 155 to 200 of Figure 8 the standard deviation is low and more or less constant, these rows show the background and the tube wall in the images and the standard deviation there is not influenced by the flow in the tube.

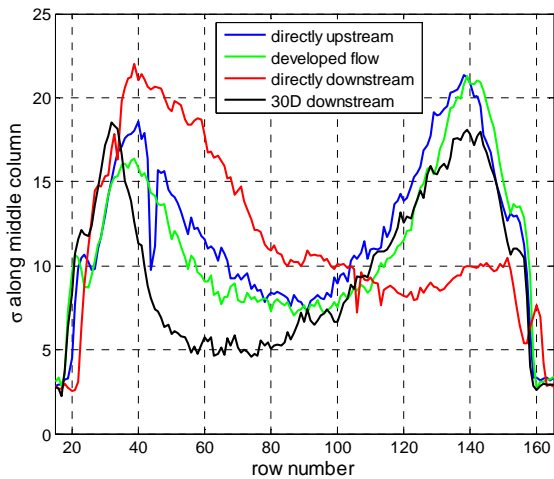


Figure 8 Standard deviation along columns Figure 7
(---)

The differences in the standard deviations and thus in the flow behaviour are immediately apparent. As already shown in Figure 7, the difference between the flow behaviour directly upstream and the fully developed flow 30 diameters upstream are indeed very minor. They are easily explained by small deformations of the image due to being recorded at a different position along the hairpin. The flow visualizations on which these two standard deviation profiles were calculated were recorded on positions more than 100D away from each other along the hairpin. The fact that the differences between them are so minor shows that this same standard deviation profile would be found in any location along the tube if tube would be straight and the flow behaviour would be undisturbed. The flow directly downstream of the U-bend shows a significantly smaller standard deviation at rows 100 to 150, this is from the middle to three quarters down of the image. This deviation is almost fully restored 30 diameters downstream. Near the top of the tube, rows 50 to 100, the standard deviation is significantly higher than in the fully developed case. Thirty diameters downstream the standard deviation is actually lower in this zone, which shows that the flow is still undeveloped. To determine the development length downstream of the U-bend, measurements should be taken even further downstream, which was not possible with the current setup.

In conclusion, the flows recorded 30 diameters downstream from the U-bend still showed significant differences compared

to the fully developed flow for all three observed flow regimes. This indicates that the flow is still not fully developed after 30 diameters. This is in agreement with the findings of Cho and Tae [14] and da Silva Lima and Thome [15], who both found that the flow needs more than 30 diameters to redevelop downstream of a (sharp) U-bend.

PRESSURE DROP MEASUREMENTS

Pressure drop has been measured at different locations as stated above. Because of the highly unsteady character of two-phase flow the pressure difference also varies in time. The pressure drop values presented below are averages taken over 10s. Taking the average over a longer time span did not affect the average value significantly. The measurements were only started if the average remained steady for at least 10 minutes.

Pressure drop measurements for fully developed flow

In Figure 9 the pressure drop measurements in the tube section where the flow is assumed to be developed (30 D upstream of the bend) are shown for different mass fluxes.

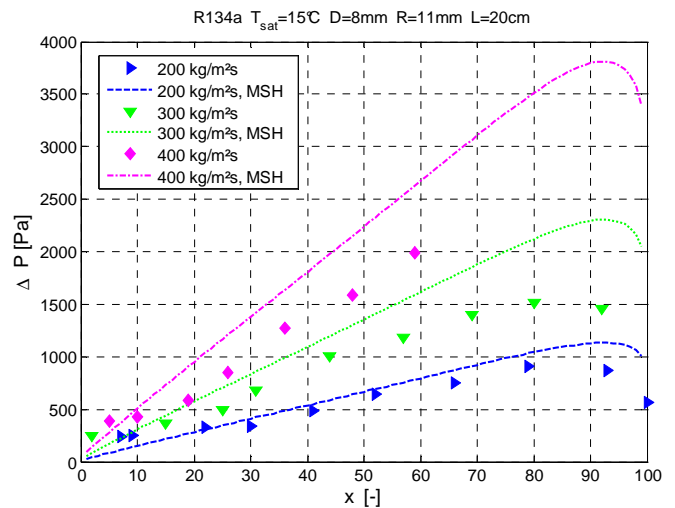


Figure 9 Pressure drop measurements in case of developed flow compared to pressure drop predictions of Müller-Steinhagen and Heck [16]

Unfortunately the setup does not allow to attain stable conditions at high G and x , so the series of $G = 400 \text{ kg/m}^2\text{s}$ is not complete. The pressure drop predicted by the Müller-Steinhagen and Heck correlation [16] is also shown in this figure.

A similar trend is seen in both the measurements and the correlation: first the pressure drop increases with vapour quality x , then it attains a maximum at a high x after which it decreases again. This trend is expected for two phase pressure drop. When the thin liquid film at these high vapour fractions starts to disappear locally, there is a reduction in the friction between the phases causing a decrease in the observed pressure drop.

Apart from a few points at low x , where the measurement uncertainty is quite large, the discrepancy is smaller than 30%. Considering the Müller-Steinhagen and Heck correlation

renders an uncertainty of more than 30%, the flow can be assumed to be fully developed in this section. In the subsequent part this measured pressure drop will be used as a reference value to assess the impact of the bend. Furthermore, Figure 9 shows that the Müller-Steinhagen and Heck correlation predicts the data for the lowest mass flux the most accurately.

Pressure drop measurements upstream of the U-bend section

In Figure 10 the pressure drop measurements recorded in the section upstream of the U-bend are shown for varying mass fluxes. Again, this data exhibits a trend similar to what is expected for two-phase flow.

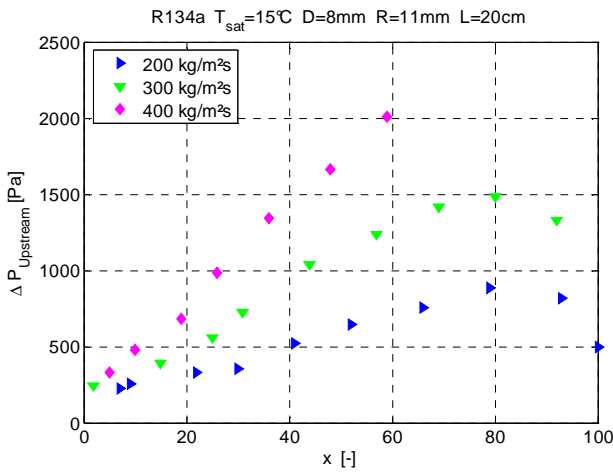


Figure 10 Pressure drop measurements in the interval immediately upstream of the U-bend

Pressure drop measurements downstream of the U-bend section

Likewise, this trend is observed in the pressure drop measurements downstream of the U-bend (Figure 11).

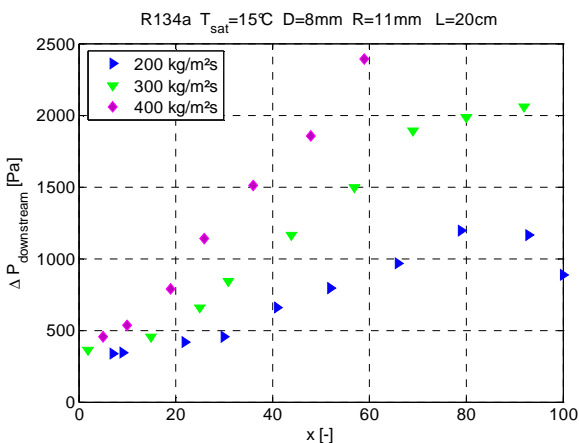


Figure 11 Pressure drop measurements in the interval immediately downstream of the U-bend

Comparing Figure 9, Figure 10 and Figure 11 shows that the pressure drop downstream of the U-bend consistently

exceeds those in case of developed flow and upstream of the U-bend.

Estimation of the U-bend effect

The ratio of the pressure drop measurements for developed flow and flow downstream of the U-bend is shown in Figure 12. As shown, the pressure drop downstream of the U-bend exceeds the pressure drop of developed flow for all data points. This difference is statistically significant. As discussed above, the flow downstream of the U-bend needs to redevelop, which explains the increase in pressure drop compared to developed flow. Indeed, in a developing flow the interfacial changes cause more friction between both phases and between the phases and the inner tube wall.

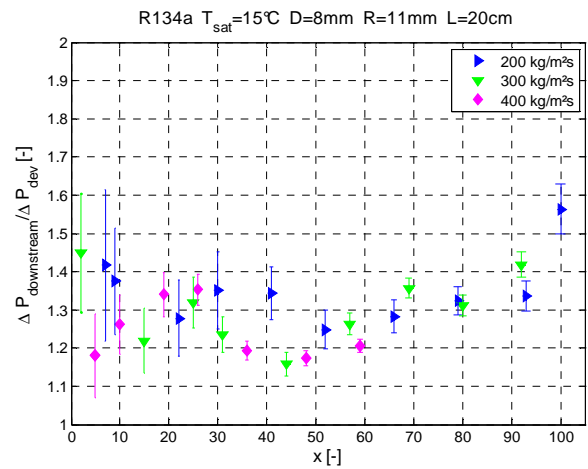


Figure 12 Ratio of the pressure drop downstream of the U-bend and pressure drop for developed flow

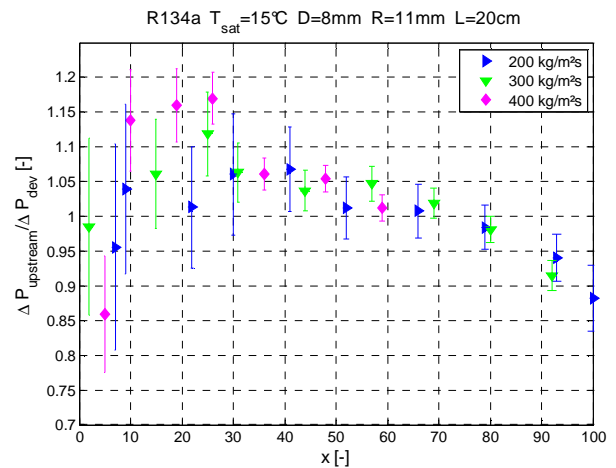


Figure 13 Ratio of the pressure drop downstream of the U-bend and pressure drop for developed flow

This limited dataset indicates that the ratio of the pressure drop downstream of the U-bend and pressure drop for developed flow does not show a distinctive trend in function of G and x .

It more or less fluctuates around 1.3. The ratio of the pressure drop upstream of the U-bend to that for developed flow is shown in Figure 13.

The trend observed in this ratio cannot be explained at this instant. A slight acceleration of the flow at small x and a slight deceleration at high x might be the cause. As discussed previously, no significant U-bend effects were observed on the flow behaviour upstream of the U-bend, which is also clear from Fig. 13.

CONCLUSION

Pressure drop and refrigerant flow videos have been recorded in tube sections with developed and developing flow and upstream and downstream of the U-bend of a hairpin. It was found that the pressure drop downstream of the U-bend consistently exceeds the pressure drop in case of developed flow. Comparing this to the visual observation of the flow downstream of the U-bend, one can see that the flow is clearly affected by the U-bend. This explains the observed increase in pressure drop, as the flow needs to develop again, causing more friction between both phases. Moreover, the flow is still not developed more than 30 diameters downstream of the U-bend, which leads to believe that the pressure drop will still be affected further than 30 diameters from the U-bend. Further research is needed to estimate how far the effect of the U-bend on flow and pressure drop extends.

REFERENCES

- [1] A. M. Ribeiro, T. R. Bott, and D. M. Jepson, "The influence of a bend on drop sizes in horizontal annular two-phase flow," *International Journal of Multiphase Flow*, vol. 27, pp. 721-728, 1999.
- [2] C. C. Wang, I. Y. Chen, Y. W. Yang, and Y. J. Chang, "Two-phase flow pattern in small diameter tubes with the presence of horizontal return bend," *International Journal of Heat and Mass Transfer*, vol. 46, pp. 2975-2981, 2003.
- [3] C. C. Wang, I. Y. Chen, Y. T. Lin, and Y. J. Chang, "A visual observation of the air-water two-phase flow in small diameter tubes subject to the influence of vertical return bends," *Chemical Engineering Research & Design*, vol. 86, pp. 1223-1235, Nov 2008.
- [4] C. Y. Yang and C. C. Shieh, "Flow pattern of air-water and two phase R134a in small circular tubes," *International Journal of Multiphase Flow*, vol. 27, pp. 1163-1177, 2000.
- [5] A. K. Chesters, "The applicability of dynamic similarity criteria to isothermal, liquid-gas two-phase flows without mass transfer," *International Journal of Multiphase Flow*, vol. 2, pp. 191-212, 1975.
- [6] I. Y. Chen, Y. S. Wu, J. S. Liaw, and C. C. Wang, "Two-phase frictional pressure drop measurements in U-type wavy tubes subject to horizontal and vertical arrangements," *Applied Thermal Engineering*, vol. 28, pp. 847-855, Jun 2008.
- [7] D. Chisholm, *Two-phase flow in pipelines and heat exchangers*. London: Godwin, 1983.
- [8] P. A. Domanski and C. J. L. Hermes, "An improved correlation for two-phase pressure drop of R-22 and R-410A in 180 degrees return bends," *Applied Thermal Engineering*, vol. 28, pp. 793-800, May 2008.
- [9] M. Padilla, R. Revellin, and J. Bonjour, "Prediction and simulation of two-phase pressure drop in return bends," *International Journal of Refrigeration-Revue Internationale Du Froid*, vol. 32, pp. 1776-1783, Nov 2009.
- [10] D. F. Geary, "Return bend pressure drop in refrigeration systems.," *ASHRAE Trans.*, vol. 81, pp. 250-264, 1975.
- [11] H. Caniere, B. Bauwens, C. T'Joel, and M. De Paepe, "Probabilistic mapping of adiabatic horizontal two-phase flow by capacitance signal feature clustering," *International Journal of Multiphase Flow*, vol. 35, pp. 650-660, Jul 2009.
- [12] H. Canière, "Flow Pattern Mapping of Horizontal Evaporating Refrigerant Flow Based on Capacitive Void Fraction Measurements," *Doctoraatsthesis, Universiteit Gent*, 2009-2010.
- [13] H. Canière, "Flow Pattern Mapping of Horizontal Evaporating Refrigerant Flow Based on Capacitive Void Fraction Measurements," Phd Thesis, Ghent University, Ghent, 2010.
- [14] K. Cho and S. J. Tae, "Evaporation heat transfer for R-22 and R-407C refrigerant-oil mixture in a microfin tube with a U-bend," *International Journal of Refrigeration-Revue Internationale Du Froid*, vol. 23, pp. 219-231, May 2000.
- [15] R. J. da Silva Lima and J. R. Thome, "Two-Phase Pressure Drops in Adiabatic Horizontal Circular Smooth U-Bends and Contiguous Straight Pipes (RP-1444)," *Hvac&R Research*, vol. 16, pp. 383-397, May 2010.
- [16] H. Müller-Steinhagen and K. Heck., "A simple friction pressure drop correlation for two-phase flow in pipes," *Chemical Engineering and Processing*, vol. 20, pp. 297-308, 1986.